Simplified and Systematic Design Procedure for High Frequency Wideband and Multiband Baluns

by

Rahul Gupta

Under the Supervision of Dr. Mohammad S. Hashmi

Indraprastha Institute of Information Technology Delhi

April, 2017

Indraprastha Institute of Information Technology (IIITD), New Delhi 2017

Simplified and Systematic Design Procedure for High Frequency Wideband and Multiband Baluns

by

Rahul Gupta

Submitted

in partial fulfillment of the requirements for the degree of

Master of Technology in

Electronics and Communication Engineering

to

Indraprastha Institute of Information Technology Delhi

April, 2017

Certificate

This is to certify that the thesis titled **"Simplified and Systematic Design Procedure for High Frequency Wideband and Multiband Baluns"** being submitted by ***Rahul Gupta*** to the Indraprastha Institute of Information Technology Delhi, for the award of the Master of Technology, is an original research work carried out by him under my supervision. In my opinion, the thesis has reached the standards fulfilling the requirements of the regulations relating to the degree. The results contained in this thesis have not been submitted in part or full to any other university or institute for the award of any degree/diploma.

April, 2017

Dr. M. S. Hashmi

Department of Electronics and Communication Engineering

Indraprastha Institute of Information Technology Delhi

New Delhi 110 020

Acknowledgements

This Master's Thesis has been prepared by Rahul Gupta at the Indraprastha Institute of Information Technology, Delhi, during August, 2016 – April, 2017. I would like to thank my thesis supervisor Prof. Dr. Mohammad S. Hashmi for providing me valuable advice and help during the entire period of work. This work would not have been complete without his support.

I thank Md. A. Maktoomi for providing me deeper insights of the passive RF circuits, conventional circuit solving techniques and problem solving approach. Thanks to all the authors of the papers I have referred, to the people whose webinars and lectures have helped me develop this work.

Lastly, I would like to thank my parents who have always kept enormous faith in me, have been on my side every minute of my life and blessed me with immense love. Though, a "thanks" would not be enough!

Abstract

Baluns are ubiquitous element in numerous applications such as RF/Microwave components and systems, TV receivers, and modern era telecommunication networks. These are primarily used with push-pull amplifiers, balanced mixers, and in driving the antennas. There have been several reported techniques for balun but it has been always challenging to design balun architectures with wideband and multi-frequency operations. Though, there are multiple reports on wideband and dual-band baluns, there is only one report, that too employing several compensation techniques with complex defected ground structure (DGS), which shows effective operation at three arbitrary frequencies. In this thesis, therefore, a high frequency wideband balun with a very simple and intuitive impedance matching procedure is presented. Furthermore, a design scheme to provide isolation between the output ports across the whole bandwidth is also presented. The broadband balun, although, is extremely useful but may not be able to meet the requirements of evolutions in wireless standards. Keeping this in perspective, a new structure for a passive tri-band balun, operating at three arbitrary frequencies is presented. The tri-band balun is symmetric and enables simple even- and odd-mode analysis to obtain the simplified design equations. The exciting aspect of this design is the presence of free variables which can be chosen independently to facilitate the design. All the design schemes presented in this thesis have been validated through prototypes developed on microstrip boards.

Relevant Publications

1. **R. Gupta**, M. A. Maktoomi and M. S. Hashmi, “A new high frequency balun with simplified impedance matching technique,” *IEEE Asia Pacific Microwave Conference*, New Delhi, 4 pp., Dec. 2016.
2. **R. Gupta**, A. P. Yadav and M. S. Hashmi, “Symmetric tri-band balun architecture with a systematic design procedure,” *IEEE National Conference on Communications*, Chennai, 5 pp., Mar. 2017.
3. M. A. Maktoomi, **R. Gupta**, M. H. Maktoomi, M. S. Hashmi and F. M. Ghannouchi, “A generalized multi-frequency impedance matching technique," *IEEE Mediterranean Microwave Conference*, Abu Dhabi, UAE, pp. 1-4, Nov. 2016
4. **R. Gupta**, S. Kumar, S. Kaushik, M. A. Maktoomi, and M. S. Hashmi, “A new L-shaped phase inverter design utilizing a loaded transmission line,” *IEEE MTT-S International Wireless Symposium*, Shanghai, China, Mar. 2016.
5. M. A. Maktoomi, **R. Gupta**, and M. S. Hashmi, “A dual-band impedance transformer for frequency-dependent complex loads incorporating an L-type network,” *IEEE Asia-Pacific Microwave Conference*, Nanjing, China, pp. 1-3, Dec. 2015.

Contents

CHAPTER 1

INTRODUCTION TO BALUN

1.1 Introduction:

A balun is a fundamental and important constituent of a basic communication network. Starting from feeding an antenna of a television, a balun has its applications in balanced mixers, push-pull amplifiers and local oscillator applications. The need for today's high speed, low noise data transfer, multi-band operations has driven the exigency in the advancement of the balun architecture to its performance at higher frequencies and for wideband applications. In this chapter, a balun will be defined at first which will be followed by balun's types, balun's performance parameters, different types of baluns and its properties. Finally, we will discuss the applications of baluns.

The balun is an electrical transformer which is used to transform a single ended signal into a differential ended signals [1]. Balun is an acronym for balanced to unbalanced and also referred as balanced to unbalanced impedance transformer. The unbalanced port has a reference signal as ground, whereas the balanced ports have equal magnitude with reference to the ground and opposite phase with respect to each other. A balun is a three port device, as shown in Fig. 1.1, with a matched input and differential outputs with two conditions on the output signals:

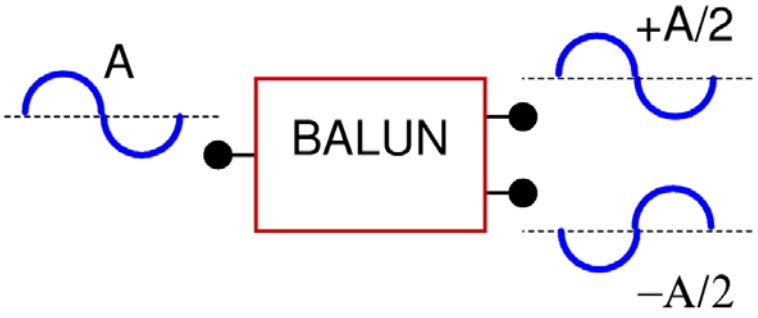

Fig.1.1 A simple balun

- The output signal should be equal in magnitude.
- The two output signals should have 180° phase difference.

These characteristics of a balun are represented by two conditions:

$$S_{11} = 0 \quad (1.1)$$

And

$$S_{21} = -S_{31} \quad (1.2)$$

Similar to a Wilkinson power divider, resistive power divider, or quadrature hybrid coupler, a balun has equal power outputs. Unlikely it has a 180° phase difference between outputs. A balun can be used as a reciprocal device that can be used bi-directionally, unlike an isolator or circulator.

1.2 Figures of Merit:

There are several parameters governing the performance of a balun. These parameters are defined below.

1.2.1 Amplitude Imbalance:

The signal available at the two output ports of a balun should be equal in magnitude. The difference in magnitude between the two output ports is known as amplitude imbalance of a balun. It is measured in dB.

Amplitude Imbalance (dB) = 20 (log S21 – log S31)

1.2.2 Phase Imbalance:

The deviation of the required 180° phase difference between the two output ports is considered as the phase imbalance. It should be as minimum as possible.

Phase Imbalance (°) = 180° - [phase (S21) - phase (S31)]

1.2.3 Insertion Loss:

It is the measure of the efficiency of a balun when it is transforming an unbalanced input signal to balanced output signal. It is the loss in the magnitude when a signal is transferred from an input port to an output port.

1.2.4 Balun Ratio/Impedance Ratio:

A balun is often used in a communication network having its application as the impedance transformer between the two

stages. This impedance ratio of the output ports to the input port is known as balun ratio or impedance ratio.

1.2.5 **Return loss:** Return loss is a measure of a balun structure for its matching abilities with a source impedance (input port) to the load impedance (output ports).

1.2.6 **Common Mode Rejection Ratio (CMRR):** This is the ratio of the differential-mode gain to the common-mode gain.

1.3 Types of Balun:

There are different category of balun in which they can be classified. It is based on the applications and based on the structures.

1.3.1 Classification Based on Applications:

1.3.1.1 **Voltage type balun:** A voltage type balun has the voltages at its output ports equal in amplitude and 180° phase apart. The voltage is induced to the secondary windings considering it as a transformer. A voltage balun may simultaneously behave as an impedance transformer.

1.3.1.2 **Current type balun:** A current type balun has the current at its output ports equal in amplitude and 180° phase apart. The Guanella balun is an example of a current balun.

1.3.2 Classification Based on Architectures:

1.3.2.1 **Flux coupled type balun:** This is a simple balun made of two electrically coupled together with wire coils around a magnetic core. The primary side (unbalanced) is connected to ground. The secondary side may have any no. of turns to keep the desired impedance ratio. This can be conventional type or auto- transformer type baluns. These types of baluns are mostly used at low frequencies and provide higher isolation.

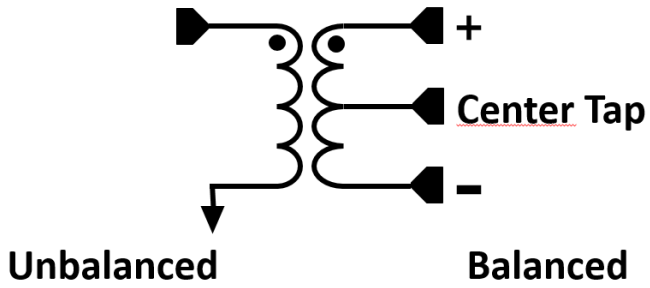

Fig. 1.2. A flux coupled type balun

1.3.2.2 **Transmission line type balun:** Transmission type baluns are made up of microstrip transmission lines. This is a set of transmission lines, sometimes coupled transmission lines with one end grounded.

Fig. 1.3. A capacitively coupled transmission line type balun

1.3.2.3 **Marchand type balun:** It is very similar to other types of transmission line type baluns. Conventional Marchand type balun consist of two quadrature wavelength coupled-line sections connected together and are grounded at the mid to create reference at the two balanced ports. These structures are realized using microstrip coupled-line because of relatively low-cost.

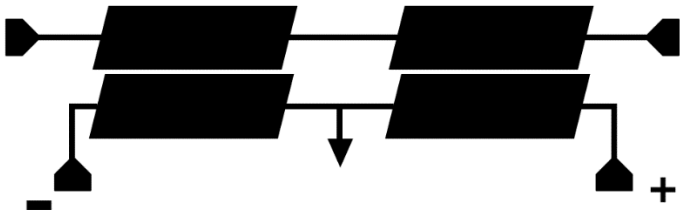

Fig. 1.3. A Marchand type balun

1.4 Applications of the Balun:

The balun is needed for various applications where impedance matching is required. It is usual while cascading any communication network. These are also required to provide isolation and to provide matching between an unbalanced port to balanced ports. Main application areas of a balun are mentioned here as follows:

a) Impedance matching networks
b) Balanced mixers
c) Push-pull amplifiers
d) Phase shifters
e) Balanced modulators
f) Coaxial antenna feeds
g) Balanced frequency multipliers

1.5 Literature Overview:

It is evident from the classification that these baluns can be operated at a particular frequency or at a range of frequencies. Though the flux coupled baluns are used for good isolation, they can only be used at the lower frequencies. Transmission line type baluns are preferred for the applications at higher bandwidth and for wideband applications. The key guidelines of balun are good matching at all its ports, insertion loss, and deviation in phase difference between the output ports.

This rapid advancement in the wireless standards and applications necessitate design and development of wideband, dual- and multi-band Balun architectures. Numerous approaches to design balun have been reported in recent past [1]-[24] and [27]. They focus on different aspects of balun design. For example, [1-4] reports baluns with wideband characteristics and [5-8] reports the marchand architecture of baluns for miniaturized structures. Being a three port device, balun architecture have poor isolation, some reports [9-10] are showing the improvement on isolation and output port matching in addition to the input port impedance matching and 180° phase difference. Another report [11] exhibits the balun performance with flexible structures. Baluns with dual-band characteristics were also proposed in [12-23]. Moreover, the design strategy for tri-band balun is still in infancy. The state-of-the art for tri-band balun architecture has very little advancements. The lone tri-band balun [24] although exhibits successful operation at the three identified frequencies, but provides relatively inferior insertion loss and deviation in requisite phase difference.

1.6 Statement of the Problem:

The main applications of a balun network in any digital communication architecture is in providing an impedance matching solution between multiple stages of the cascaded network, DC isolation and the unbalanced port matching with its balanced ports. As per the advancements in the modern era communication network, the balun is needed to be used at the multiple frequencies. These structures are also preferred to be used for wideband applications.

In this thesis, three different architectures of balun are proposed which are exhibiting wideband performance, wideband performance with isolation, and a balun working at three arbitrary frequencies respectively. The first structure is a very simplified design to provide a wideband operation at any design frequency. This structure is only catering to the basic requirements of a balun operation, i.e. input port matching and the unbalanced to balanced transformation with minimum amplitude and phase imbalance. Due to no lumped components and the applicability of the systematic design procedure,

it can be designed to high range of frequencies. Another design is the modified version of the first one with just one isolation resistor. The advantage of this design over last design is to have the adequate isolation between the two output ports. The third design proposes a tri-band balun which utilizes the concept of the feed network design [25] to offer infinite impedance at one frequency to get the performance at another frequency. A very simplified design with a systematic design procedure is presented here.

1.7 Thesis Outline:

The brief introduction of the balun is given in this chapter along with its applications. A literature overview of this chapter shows the progress in the different balun structures and then the problem statement is defined.

Chapter 2 presents the design, analysis and results of the proposed simplified wideband balun. Alongwith the systematic design procedure, this chapter also includes the comparison chart to show the improvement over the earlier reported balun. Chapter 3 represents the modified version of the design of chapter 2 with improved isolation between the two output ports. This exhibits a design with optimized bandwidth performance in addition to isolation and output ports matching for the complete bandwidth.

Chapter 4 presents the analysis and design of a tri-band balun with a systematic design procedure. This structure also doesn't use any lumped component not to limit its operation at higher frequencies. Two design examples at different frequency ratios are calculated to verify the wide range applications of the proposed structure. Finally, the design results are compared with the earlier reports and it claims favorably better response. At the end, conclusion and references are included.

CHAPTER 2

A NEW HIGH FREQUENCY BALUN WITH SIMPLIFIED IMPEDANCE MATCHING TECHNIQUE

2.1 Introduction:

In this chapter, a high frequency balun with a very simple and intuitive impedance matching procedure is presented. Owing to the presence of symmetry in the proposed structure, the even-odd mode analysis is applied which results into closed-form design equations. Since, the proposed design has many variables that can be chosen independently, the design equations are investigated to assess the limitation of the choice of different variables. Based on the proposed theory, a balun has been designed for operation at 2 GHz and implemented on RO4350B substrate. The EM simulation and the measured results match well and thus validate the design.

2.2 Analysis and Design of the Proposed Balun:

The complete schematic of the proposed balun is shown in Fig. 2.1. This 3-port network is obtained by leaving the one port of a conventional four port branch-line structure open. Since, this structure has symmetry about XX'-axis, and therefore, the even odd-mode analysis can readily be applied for the deduction of the design equations. A balun is described by the following set of equations involving transmission T or impedance Z [11]:

$$T_{even} = 0 \tag{2.1}$$

$$Z_{odd} = 2Z_0 \tag{2.2}$$

$$Z_{even} = 0 \tag{2.3}$$

That is, signal must not be able to flow in the even-mode while the odd-mode input impedance must be equal to twice that of the port impedance, Z_0. Since, the first condition can be achieved by somehow forcing a signal ground at the input port, theref-

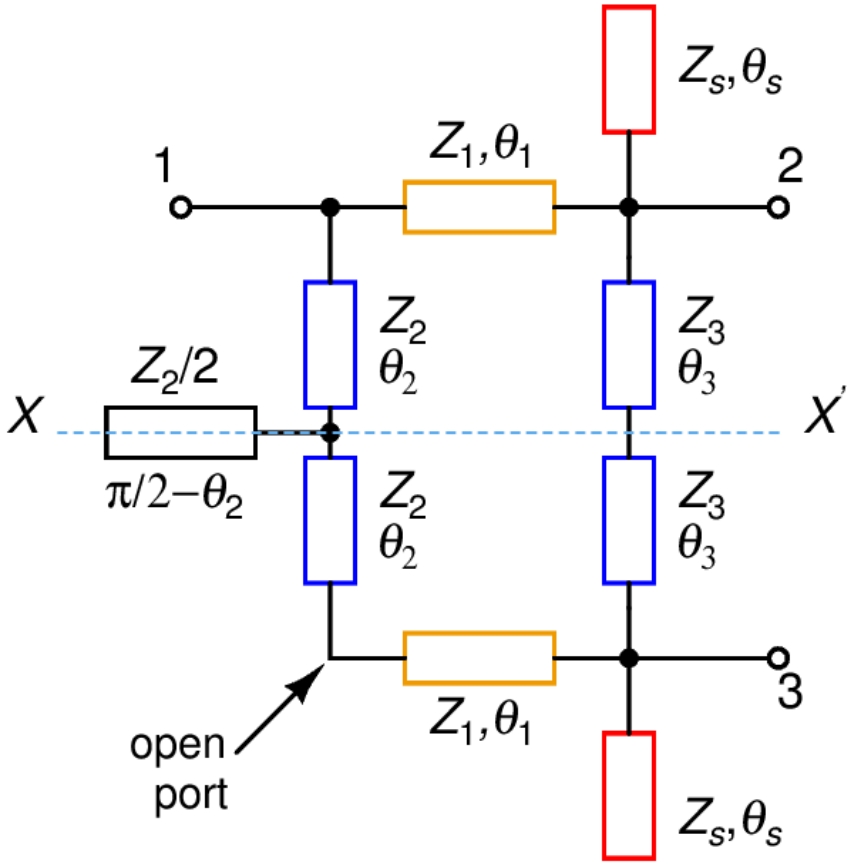

Fig. 2.1. The proposed tri-band balun

ore, the same can also be stated as equation (2.3).

The even-mode equivalent circuit of the proposed balun is obtained by considering every point along the XX'-axis as open-circuited as shown in Fig. 2.2, where Z_{even} is the impedance looking to the right in this mode. Since, the total length of the open stub at the node n_2 is chosen to be $\theta_2 + \pi/2 - \theta_2 = \pi/2$; a virtual short appears at the node n_2 due inverse property of a quarter wavelength stub. Since, this short circuit

will not be impacted upon by the rest of elements, therefore, $Z_{even} = 0$, that is, there is no signal transmission past the node n_2.

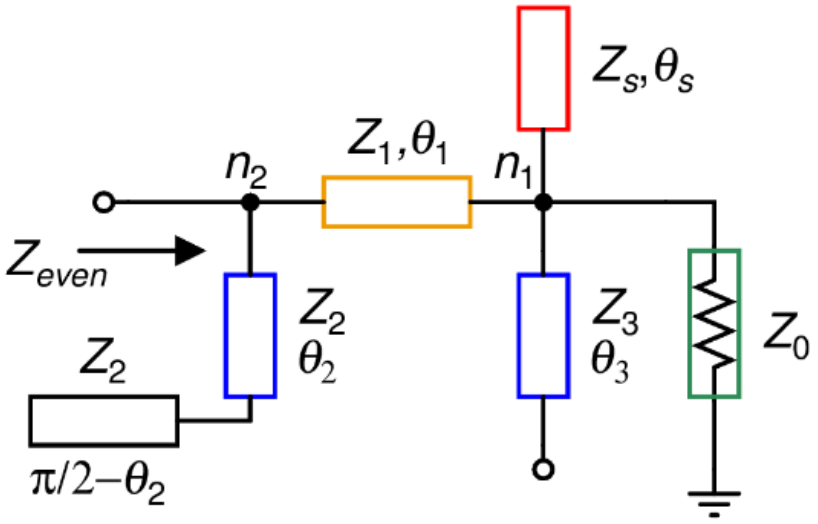

Fig. 2.2. The even-mode equivalent circuit of the balun.

In addition, each point on the XX'-axis in Fig. 2.1 is short during the odd-mode decomposition, therefore, the circuit shown in Fig. 2.3 (a) represents the odd-mode equivalent of the proposed balun. At the node n_1, the function of the upper open-circuited stub having admittance Y_a is to cancel the effect of the lower short-circuited stub with admittance Y_b. It implies

$$\frac{\tan\theta_s}{Z_s} - \frac{\cot\theta_3}{Z_3} = 0 \tag{2.4}$$

and, therefore,

$$Z_s = \frac{\tan\theta_s}{\cot\theta_3} Z_3 \tag{2.5}$$

Ensuring $Y_a+Y_b = 0$ also means that the two stubs are out of the scene and thus, $Z_r = Z_0$ and simplified odd-mode equivalent circuit is shown in Fig. 2.3 (b), which is a simple L-type network. It is this simplicity that emanates from using the extra stub which is otherwise not possible in the earlier reported design [11].

Now, in Fig. 2.3 (b), Y_{r2} is the admittance looking to the right of the node n_2 and is expressed as follows:

$$Y_{r2} = G_{r2} + jB_{r2} \tag{2.6}$$

where,

$$G_{r2} = \frac{Z_0\left(1+\tan^2\theta_1\right)}{Z_0^2 + Z_1^2\tan^2\theta_1} \tag{2.7}$$

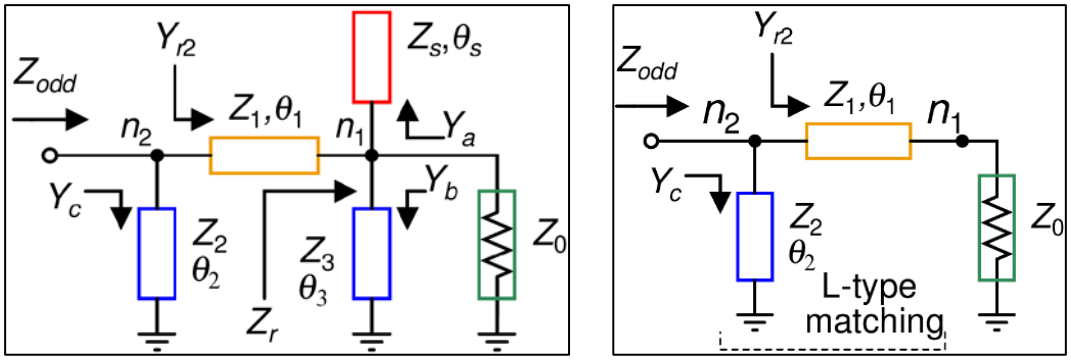

(a) (b)

Fig 2.3. (a) Odd mode equivalent of the proposed circuit and (b) simplified odd mode equivalent

and,

$$B_{r2} = \frac{\left(Z_0^2 - Z_1^2\right)\tan\theta_1}{Z_1\left(Z_0^2 + Z_1^2\tan^2\theta_1\right)} \tag{2.8}$$

Now, Y_c is used to cancel the imaginary part of Y_{r2}, that means:

$$Y_c + jB_{r2} = 0 \tag{2.9}$$

$$\Rightarrow Z_2 = \cot\theta_2 / B_{r2} \tag{2.10}$$

According to (2.2), the left-over real part of Y_{r2} must be given as follows:

$$G_{r2} = 1/2Z_0 \tag{2.11}$$

Substituting G_{r2} from (2.7) into (2.11) yields:

$$\Rightarrow Z_1 = \sqrt{\frac{Z_0^2\left(1+2\tan^2\theta_1\right)}{\tan^2\theta_1}} \tag{2.12}$$

It must be noted that the design equations have been obtained for Z_1, Z_2 and Z_s only, and therefore, the rests of the variables can be chosen independently. This does reflect flexibility of the proposed network. However, one must select these variables very judiciously. For example, it is apparent from (2.12) that Z_1 is always greater than Z_0. It

results in $B_{r2}<0$ if $\theta_1<\pi/2$ and since, Z_2 must be positive, it would require a $\theta_2>\pi/2$. But, θ_2 cannot exceed $\pi/2$ else the length of the stub with characteristic impedance $Z_2/2$ would become negative. And, therefore, θ_1 must be chosen to be greater than $\pi/2$. It is apparent from (2.5) and (2.9) that the sign of B_{r2} depends on the fact that whether $\theta_1>\pi/2$ or $\theta_1<\pi/2$, but that of Z_1 is independent of this fact. Moreover, the independent variables must be selected in a manner such that Z_1, Z_2, Z_3 and $Z_s \in [20\Omega, 140\Omega]$ in all cases so that the balun could be physically realized in microstrip.

2.3 Design Procedure and Design Example:

Keeping the above mentioned points in mind, the design steps of the proposed balun may be summarized as follows:

a) Appropriate values of θ_1, θ_3, θ_s, and Z_3 are chosen. Z_3 must be chosen between 20Ω to 140Ω. Using these values, Z_s is then determined from (2.5) and Z_1 is determined from (2.12).

b) Using the value of Z_1 found in the previous step, B_{r2} is determined from (2.8).

c) A value of θ_2 is chosen that leads to the value of Z_2 form (2.10).

Based on the design procedure outlined in the last section, a balun is designed to work at 2 GHz. Z_3 is selected as 90Ω and $\theta_3 = \theta_s = 45°$ is chosen. It results into $Z_s = 90\Omega$. Since, θ_1 is required to be greater than 90°, therefore, it is conveniently chosen as 120°. This results into Z_1=76.38Ω. Finally, choosing θ_2=70°, Z_2 is found to be 96.3Ω.

2.4 Simulation and Measurement Results:

The simulation results of the designed balun using ideal transmission line elements are shown in Figs. 2.4. It is apparent that the design has the characteristic of a balun with very good matching at port-1 at the chosen frequency of 2 GHz with extremely good transmission characteristics. The phase shift of 180° @2 GHz should also be evident in Fig. 2.4 (b).

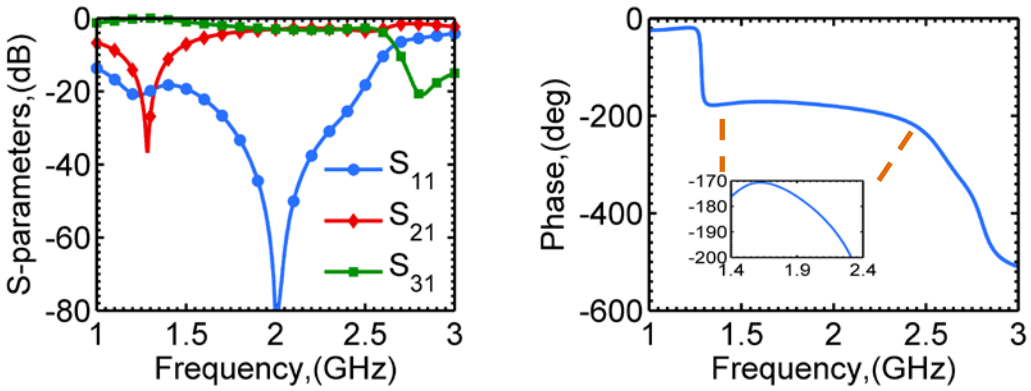

(a) (b)

Fig. 2.4. (a) Simulated (ideal) S-parameters of the designed balun. (b) Simulated (ideal) phase difference of the designed balun.

The designed balun is implemented on RO4350B substrate with ϵ_r = 3.48, $tan\delta$ = 0.003 and substrate-height of 1.5mm. The copper-cladding is 35µm on both the sides of the laminate. Since, there are corners/junctions in the proposed balun; the final design was optimized to take these discontinuities into account. Especially, the phase-difference was optimized to be a bit flatter. The fabricated device is shown in Fig. 2.5 while the EM (electromagnetic) simulation and the measured results are given in Fig. 2.6. It is apparent that the optimization has changed the S-parameters and phase response, but all of them are within permissible limits. The maximum phase deviation is ±5° from the ideal value of 180° within the bandwidth of 1.7 GHz to 2.2 GHz (=500 MHz).

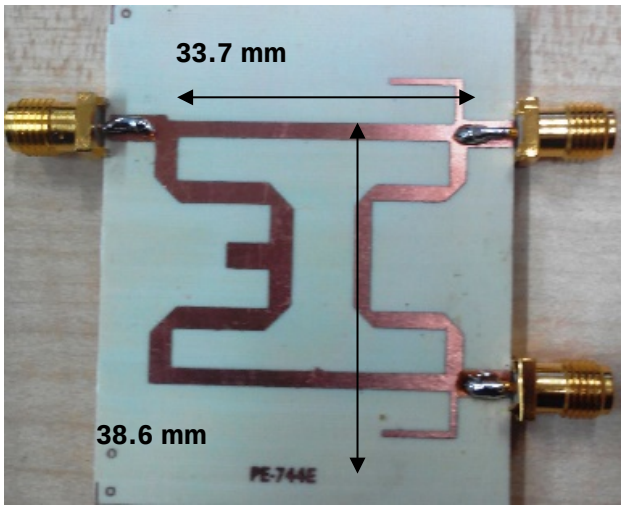

Fig. 2.5. The fabricated balun on RO4350B substrate.

Finally, comparison with an earlier and the latest reported design given in Table 2.1 shows the overall the presented scheme exhibit good performance.

TABLE2.1 COMPARISION WITH [11]

Ref.	Parameters		
	Total Perimeter	*BW (%)*	*Return loss (dB)*
[11] Type-I	$1.3\lambda_0$	15	>30
[11] Type-II	$0.9\lambda_0$	10.6	>40
This Work	$1.03\lambda_0$	25	>30

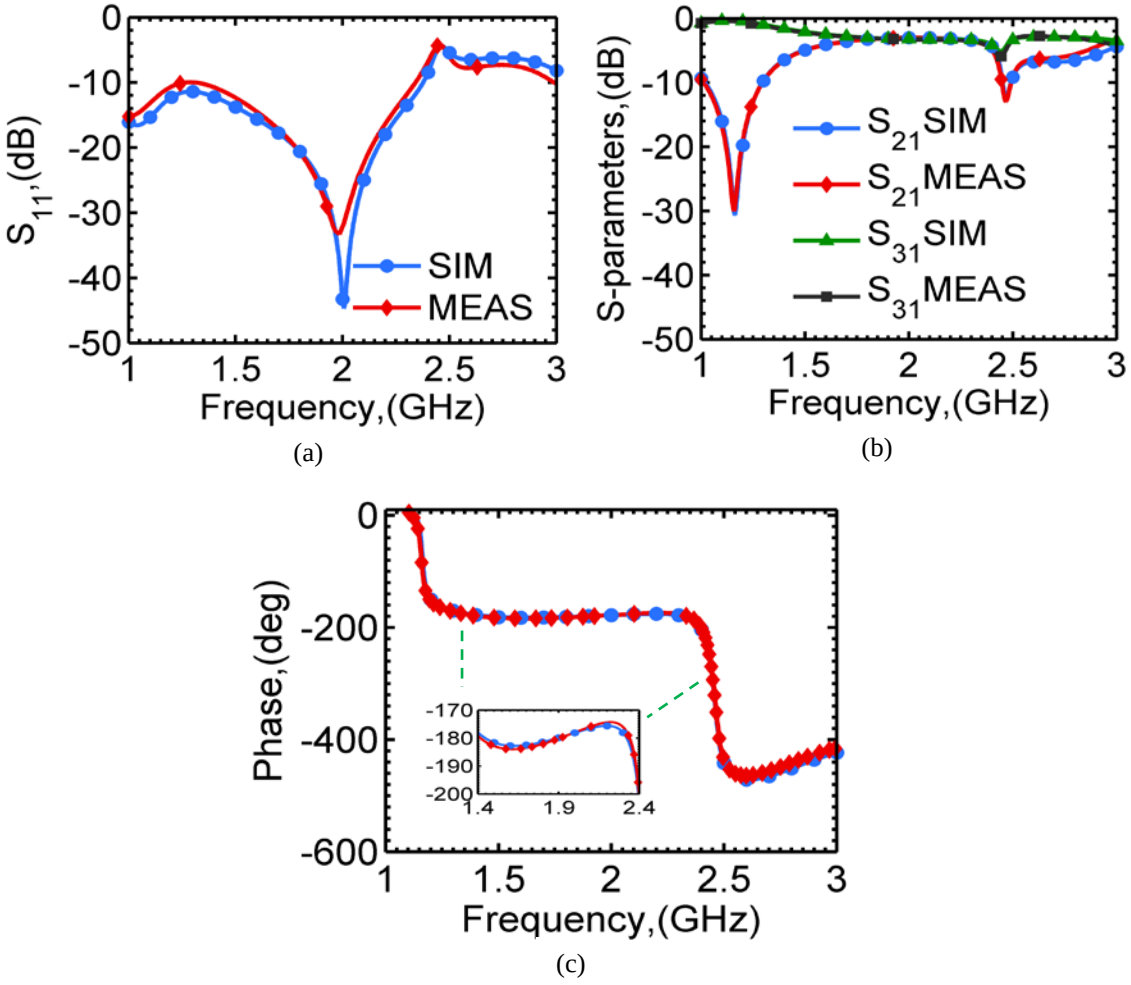

Fig. 2.6. Simulation (EM) and measured results of the designed device (a) Return-loss, (b) transmissions, and (c) phase difference.

2.5 Conclusion:

A new structure of high frequency balun has been proposed in this chapter. The idea is to simplify the matching used in the conventional balun. Very intuitive explanation of its working has been given, and closed-from design equations have also been obtained using the even-odd mode analysis technique. A balun prototype has also been designed based on the outlined design procedure and its measurement and simulation results have been found to be in good agreement.

CHAPTER 3

SIMPLIFIED APPROACH TO DESIGN A WIDEBAND BALUN WITH OUTPUT PORTS MATCHING AND ISOLATION

3.1 Introduction:

In this chapter, the wideband balun proposed in the last chapter is modified to cater the need of the isolation between the output ports. Though it is not necessary to have the matching and isolation at the output ports of a balun for its proper operation, there are reports [1], [6], [9-10], [19-20], [23] and [27] presented to improve the balun performance on these parameters. Keeping the architecture and its systematic analysis very similar as of the simplified balun in the last chapter, the design leads to improve the isolation between the two output ports. The same approach of even-odd mode analysis is applied which results into closed-form design equations. Based on the proposed theory, a balun has been designed for operation at 1.8 GHz and implemented on RO5880 substrate. The EM simulation and the measured results match well and verify the working of the proposed design.

3.2 Analysis and Design of the Proposed Balun:

The architecture of the proposed balun is shown in Fig. 3.1. This 3- port network remains symmetrical along the axis xx' considering the fourth port of this architecture as open. All the transmission line characteristic impedances are in Ω and are denoted by Z_i and the electrical lengths are in degrees (°) and are denoted by θ_i where i=1,2,..,5. Here, Z_5=$Z_4/2$ and $\theta_5 = \pi/2 - \theta_4$. All the ports are considered to be terminated with

impedance Z_o. Utilizing the conditions mentioned in (3.1), and (3.2) for the proper operation of a balun, the proposed architecture is analyzed in this chapter.

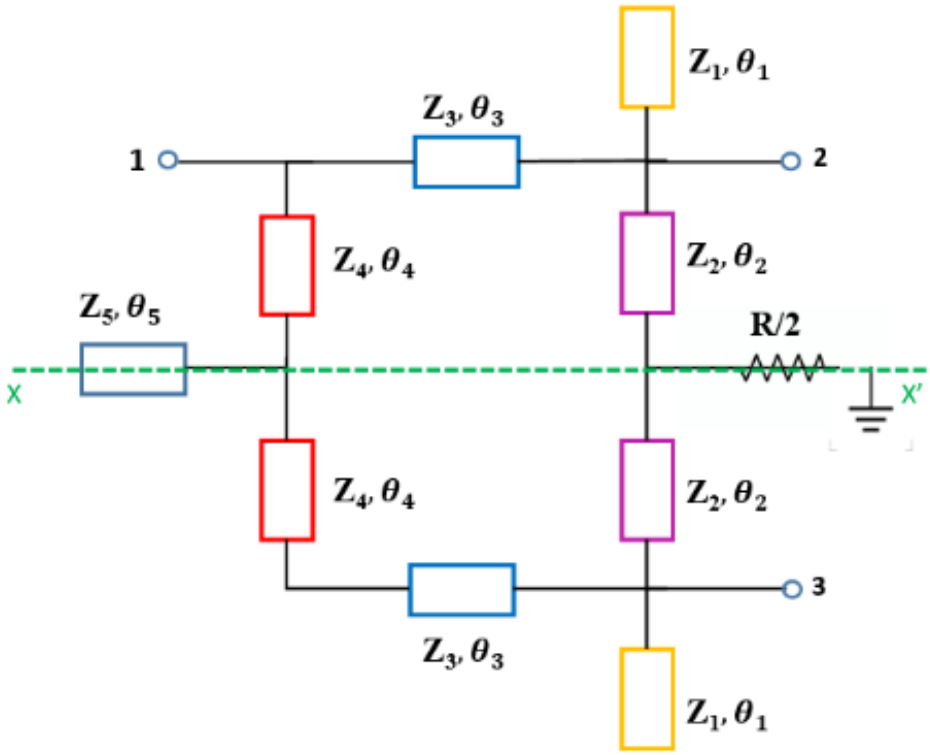

Fig. 3.1. The proposed tri-band balun

$$T_{even} = 0 \tag{3.1}$$

$$Z_{odd} = 2Z_0 \tag{3.2}$$

3.2.1 Even Mode Analysis:

In the even mode analysis, all the junctions along the xx' axis will be open circuited as shown in Fig. 3.2 (a), where Z_{even} is the impedance looking to the right in this mode. It is known that due to the symmetry of the proposed planar balun, the relationship $S_{33}=0$ and $S_{23}=0$ are naturally established when $S_{22}=0$ [27]. The even mode analysis of the architecture is done similarly as in the previous chapter. Since, the total length of the open stub at the node a_1 is $\theta_4 + \theta_5 = \theta_4 + \pi/2 - \theta_4 = \pi/2$; a virtual short appears at the node a_1 due to an open circuited quarter wavelength stub. This short circuit at node a_1 forces the input impedance to zero and therefore, $Z_{even} = 0$, that is, no signal transmission at the input port.

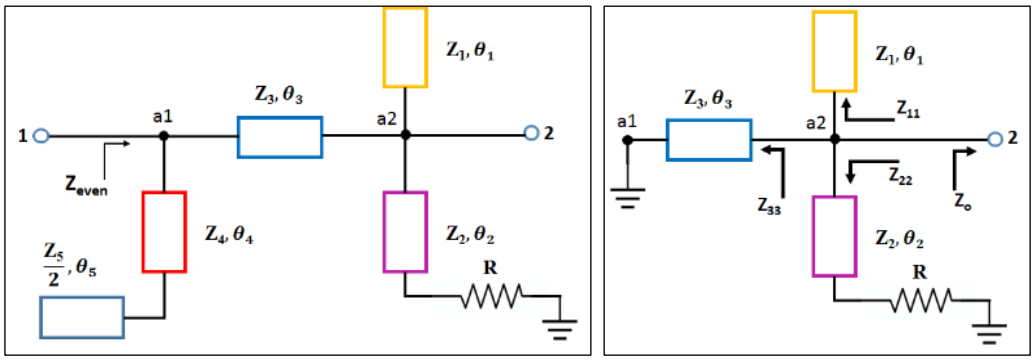

(a) (b)

Fig. 3.2 (a) The even-mode equivalent circuit of the proposed balun and (b) Simplified circuit of the even mode equivalent

This short circuit at the input port transforms the even mode equivalent circuit as shown in Fig. 3.2 (b).Here, Z_{11}, Z_{22}, and Z_{33} are representing the respective input impedance while Z_o is the output port impedance that is considered equal to the input port impedance. Hence, for the output port matching,

$$\frac{1}{Z_o} = \frac{1}{Z_{11}} + \frac{1}{Z_{22}} + \frac{1}{Z_{33}} \tag{3.3}$$

Where,

$$Z_{11} = \frac{Z_1}{j \tan\theta_1} \tag{3.4}$$

$$Z_{22} = Z_2 \frac{R + j Z_2 \tan\theta_2}{Z_2 + j R \tan\theta_2} \tag{3.5}$$

$$Z_{33} = jZ_3 \tan\theta_3 \tag{3.6}$$

3.2.2 Odd Mode Analysis:

In the odd mode analysis, all the junctions along the xx' axis will be short circuited and the odd mode equivalent of the proposed design is shown in Fig. 3.3 (a). Here, Z_{odd} is the impedance looking to the right in this mode. At the node a_2, the function of the upper open-circuited stub having admittance Y_a is to cancel the effect of the lower short-circuited stub with admittance Y_b.

Hence,

$$\frac{\tan\theta_1}{Z_1} - \frac{\cot\theta_2}{Z_2} = 0 \tag{3.7}$$

And therefore,

$$Z_1 = Z_2 \tan^2\theta_1 \quad \text{for } \theta_1 = \theta_2 \tag{3.8}$$

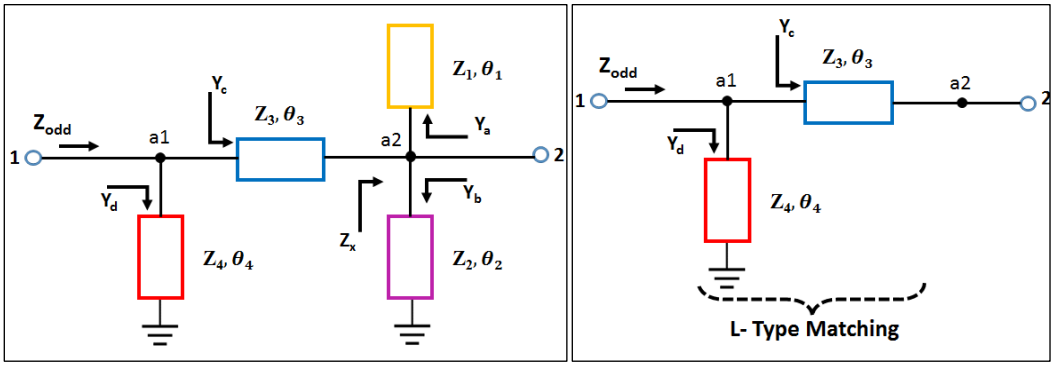

(a) (b)

Fig. 3.3 (a) The odd-mode equivalent circuit of the proposed balun and (b) Simplified circuit of the odd mode equivalent

Ensuring $Y_a+Y_b = 0$ eliminates the role of these two stubs at node a_2 and the simplified circuits is represented in Fig. 3.3 (b). The effective L-network is now used as an impedance transformer and will satisfy the requirement of (3.2). The admittance looking to the right of node a_1 can be represented as

$$Y_c = G_c + j\,B_c \tag{3.9}$$

Where, $$G_c = \frac{Z_o(1+\tan^2\theta_3)}{Z_o^2+Z_3^2\tan^2\theta_3} \tag{3.10}$$

And $$B_c = \frac{(Z_o^2-Z_3^2)\tan\theta_3}{Z_3(Z_o^2+Z_3^2\tan^2\theta_3)} \tag{3.11}$$

Now, Y_d is used to cancel the imaginary part of Y_c, that means:

$$Y_d + j\,B_c = 0 \tag{3.12}$$

$$Z_4 = \cot\theta_4 / B_c \tag{3.13}$$

And according to (3.2), putting, $G_c = 1/2Z_o$

$$Z_3 = \sqrt{\frac{Z_o^2(1+2\tan^2\theta_3)}{\tan^2\theta_3}} \tag{3.14}$$

The value of isolation resistor can now be computed using (3.3) and (3.8) and the expression for R is

$$R = \frac{Z_1 Z_o \cot\theta_1}{Z_3\tan\theta_3} \tag{3.15}$$

The expressions to obtain the values of R, Z_3, Z_4 and Z_1 only, are deduces and henceforth, the rest of the variables can be chosen independently. This does reflect the flexibility of the proposed network. However, the value of R must remain positive.

In (3.15), the values of Z_o, Z_1, and Z_3 are always positive keeping them within the realizable limit, i.e. [20Ω to 140Ω], the values of θ_1 and θ_3 must be chosen accordingly.

3.3 Design Procedure and Design Example:

The design procedure of the proposed balun along with isolation resistor can be described in brief as follows:

a) Choose the values of θ_1, θ_2, and Z_2. Z_2 must have its value between 20Ω to 140Ω. Using these values, Z_1 is then determined from (3.8) and Z_3 is determined from (3.14).
b) Determine R using (3.15). Remember the condition to keep R positive. Choose θ_3 accordingly to be greater or less than $\pi/2$.
c) From the calculated values of Z_3 and θ_3, determine B_c using (3.11). Depending on the positive or negative value of B_c, θ_4 is now chosen to calculate Z_4 form (3.13).
d) Henceforth, the values of Z_5 and θ_5 are calculated considering $Z_5=Z_4/2$ and $\theta_5 = \pi/2 - \theta_4$. To keep θ_5 positive, use $\theta_5 + \theta_4 = (2n+1)\,\pi/2$.

A design example, working at 1.8 GHz is shown here based on the above design procedure. All the port impedances are considered to be terminated with 50Ω. As θ_1, θ_2 and θ_3 are free variables here and hence chosen to be 45° at the designed frequency i.e. 1.8 GHz. Z_2 is selected as 60Ω to be between 20Ω to 140Ω to keep it in realizable limits to design it on a microstrip line. Hence Z_1 is calculated as 60Ω using (3.8) while Z_3 is calculated as 86.6Ω using (3.14). Once, Z_1 and Z_3 are known, R is computed as 23.2Ω from (3.15) and to keep its value positive, θ_3=45° is chosen. Now Z_4 = 63.4Ω and θ_4=109.9°. This results into Z_5 = 31.86Ω and θ_5=151.9°.

3.4 Simulation and Measurement Results:

The proposed architecture is simulated in a simulation environment provided by Keysight ADS based on the design values obtained in the design procedure. The design is then simulated and the EM simulation results are shown in the Fig. 3.4. Fig 3.4 (a) shows

the input port matching and insertion loss of the design and Fig. 3.4 (b) represents the isolation along with the matching at its output ports whereas Fig. 3.4 (c) shows the phase imbalance response of the balun. It is apparent from the results that the design is following the proper behavioral conditions of a balun favorably.

The designed balun is prototyped on a Rogers RO5880 substrate with ϵ_r = 2.2, $tan\delta$ = 0.0009, and substrate-thickness of 1.575 mm. The copper-cladding on both the sides of the substrate is 35µm. The fabricated prototype is shown in Fig. 3.5 with the size 57mm x 63mm. The prototype measurement results are compared with simulation results and are found to be well matched. These results are also shown in Fig. 3.4.

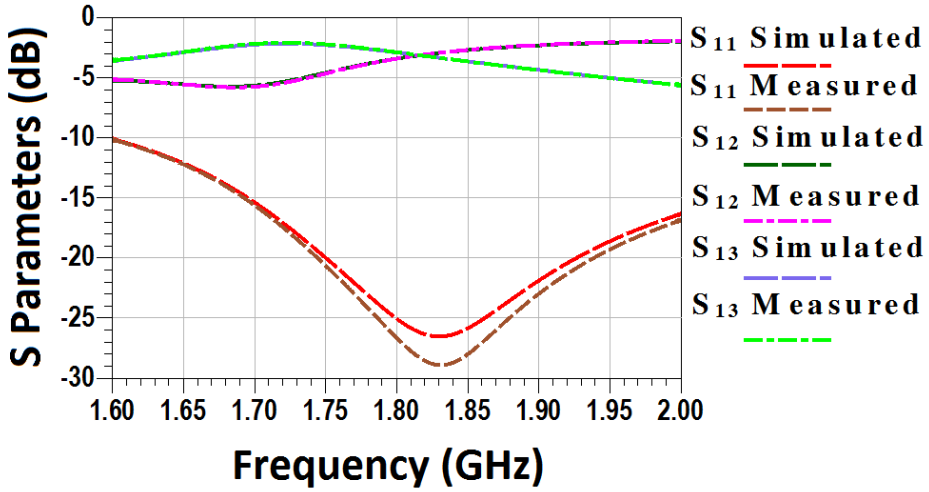

(a)

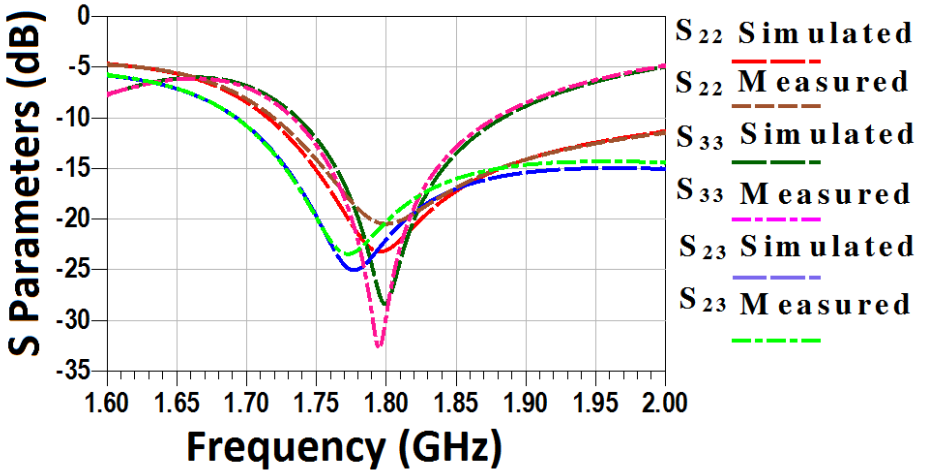

(b)

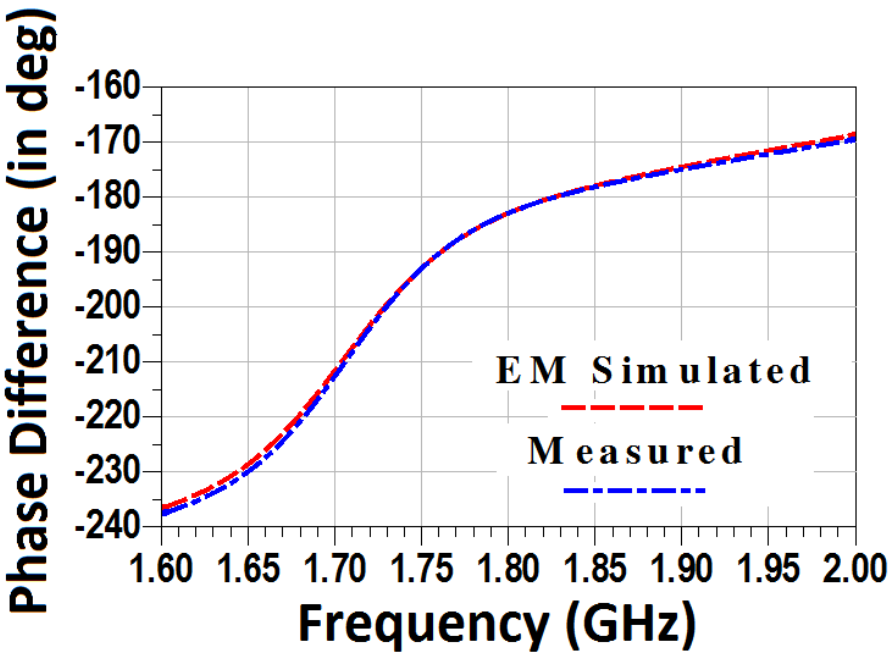

(c)

Fig. 3.4. EM Simulated vs Measurement Results of the prototype (a) Return loss and Insertion loss (b) Isolation between output ports and Output ports matching (c) Phase Imbalance

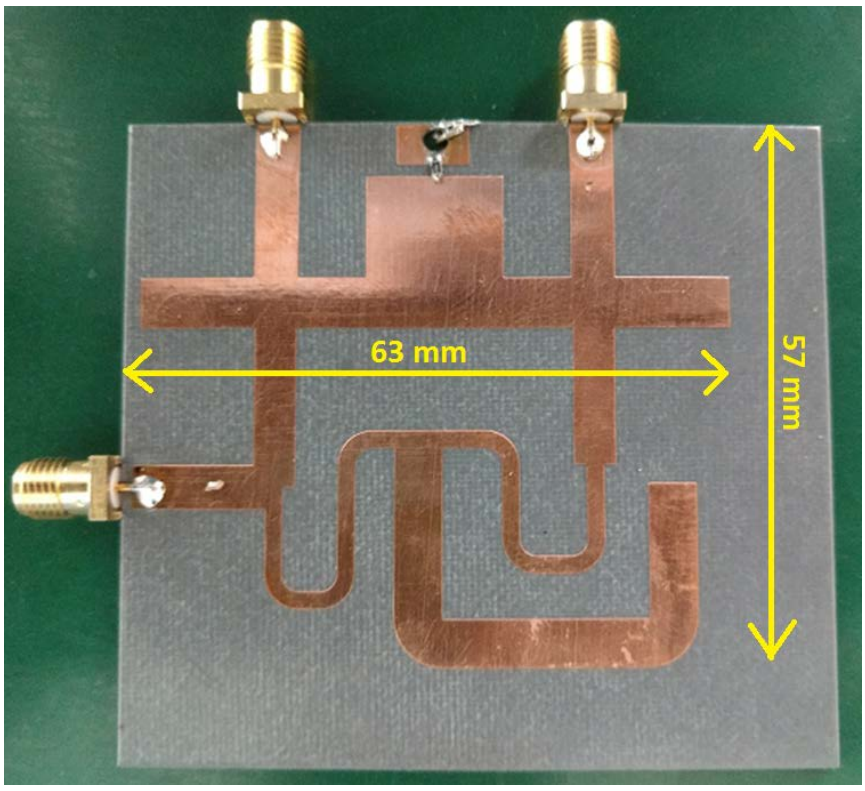

Fig. 3.5. The fabricated balun on RO4350B substrate.

Finally, comparison with an earlier and the latest reported design given in Table 3.1 shows that the overall presented scheme exhibit optimized performance.

TABLE 3.1 COMPARISION WITH [11]

Ref.	Parameters						
	Center Frequency (GHz)	***Total Perimeter***	***BW (%)***	***Return loss (dB)***	***Phase(S_{21}-S_{31}) (°)***	***Output Ports Matching (dB)***	***Isolation (dB)***
[11] Type-I	1	$1.3\lambda_0$	14.8	>30	±3	N.A.	N.A.
[11] Type-II	1	$0.9\lambda_0$	10.6	>40	±3	N.A.	N.A.
[2]	1.39	$1.23\lambda_0$	96	>40	±5	N.A.	N.A.
[1]	2.6	$2.08\lambda_0$	38	~23	±10	~15	>20
[23]	2.45 and 5.25	$1.63\lambda_0$	8.4 and 3.1 (dual band)	<20	±3	~15	N.A.
This Work	1.8	$1.4\lambda_0$	13.8	>25	±10	< -20	>20

3.5 Conclusion:

A new structure of high frequency balun has been proposed in this chapter with the improved isolation. The idea is to maintain the simplicity of the balun design as in the conventional balun. Very intuitive explanation of its working has been given, and closed-from design equations have also been obtained using the even-odd mode analysis technique. A balun prototype has also been designed based on the outlined design procedure and its measurement and simulation results have been found to be in good agreement.

CHAPTER 4

SYMMETRIC TRI-BAND ARCHITECTURE WITH A SYSTEMATIC DESIGN PROCEDURE

4.1 Introduction:

In this chapter, design of a new tri-band balun without utilizing any lumped component is proposed. This structure is initiated from a general structure of a symmetric single or dual-band balun and also retains the property of symmetry. A step-by-step even-odd mode analysis of the structure provides a very intuitive design procedure and that also aids in deducing the simplified closed form design equations. The design equations possesses free design variables and this enables it to be applicable for arbitrary chosen three frequencies. The equations also allow the easy tuning of the parameters under realizable limits (for example, it is readily accepted that the realizable characteristic impedance in microstrip technology lies between 20Ω to 140Ω). The next sections provide the background theory, analysis, design examples, prototype development and the measurement results.

4.2 Design of the Proposed Circuit:

The proposed circuit diagram of the tri-band balun network alongwith the corresponding characteristic impedances and electrical lengths is shown in Fig. 4.1. All the electrical lengths are defined at the first design frequency. The architecture is cascaded version of a dual-band balun with additional transmission lines and stubs to cater to the third arbitrary frequency. This is a symmetrical four port network in which the fourth port, i.e. Port 4, is open circuited. Now, the electrical length of the

transmission lines of dual-band section (inside the black box in Fig. 4.1) follows for dual-band operation of the network, where *i* = 3,4,5,6 and *n* = *0,1,2..,n*. The port impedance for all the ports is considered as Z_0.

$$t_i = \frac{(1+n)\pi}{1+\frac{f_2}{f_1}} = t \tag{4.1}$$

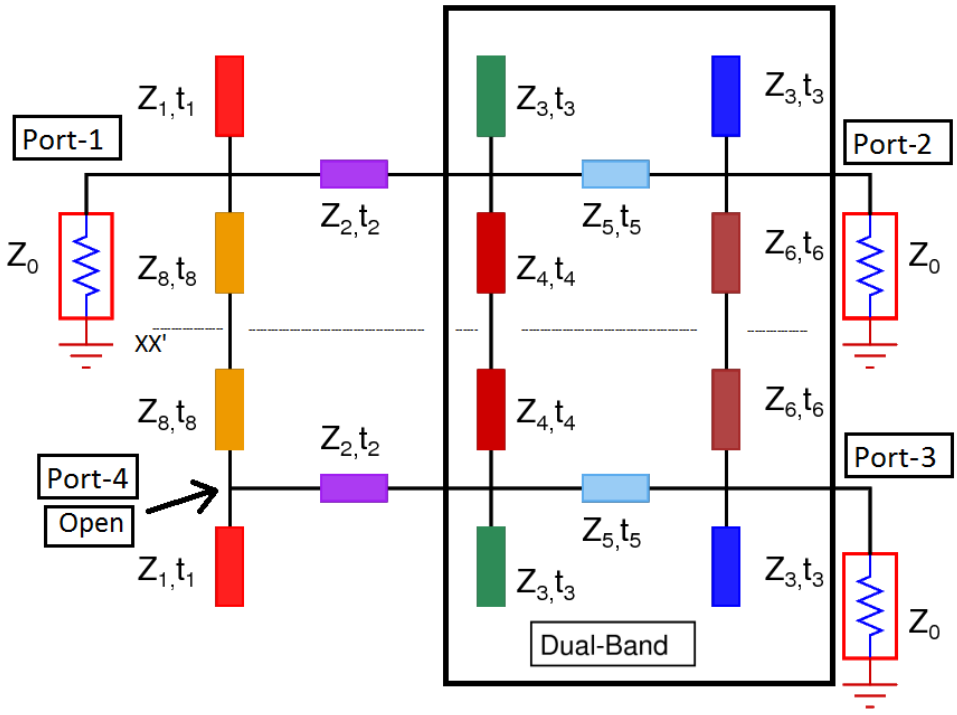

Fig 4.1. The proposed tri-band balun architecture

4.3 Analysis of the Proposed Design:

Utilizing the symmetric property of the tri-band balun, the even-odd mode technique is considered for circuit analysis. The odd-mode circuit of the tri-band balun network is shown in Fig. 4.2 whereas the even-mode circuit is shown in Fig. 4.3. A balun satisfies the following conditions for proper operation:

$$Z_{odd} = 2Z_0 \tag{4.2}$$

$$T_{even} = 0 \tag{4.3}$$

Where, Z_{odd} is the odd-mode input impedance and T_{even} = 0 indicates that the balun must not pass a signal in even-mode i.e. Z_{even} = 0.

4.3.1 Odd Mode Analysis:

In Fig. 4.2, the input admittance for the dual-band operation, Y_{odd1}, can be written as a complex expression as (4.4) where G_1 and B_1 are expressed in (4.5) and (4.6).

$$Y_{odd1} = G_1 + j\,B_1 \tag{4.4}$$

$$G_1 = \frac{[Y_5]\left[Y_0Y_5\tan^2 t + Y_0Y_5\tan^4 t\right]}{[Y_5\tan t + Y_6\tan t - Y_3\tan^3 t]^2 + Y_0^2\tan^4 t} \tag{4.5}$$

$$B_1 = \frac{[Y_5]\left[Y_3Y_5\tan^3 t + 2Y_3Y_6\tan^3 t - Y_0^2\tan^3 t - Y_3^2\tan^5 t + Y_5^2\tan^3 t - Y_3Y_5\tan^5 t + Y_5Y_6\tan^3 t\right]}{[Y_5\tan t + Y_6\tan t - Y_3\tan^3 t]^2 + Y_0^2\tan^4 t}$$
$$- \frac{Y_5Y_6\tan t - Y_6^2\tan t}{[Y_5\tan t + Y_6\tan t - Y_3\tan^3 t]^2 + Y_0^2\tan^4 t} + Y_3\tan t - \frac{Y_4}{\tan t} \tag{4.6}$$

Owing to the equation (4.2), the following condition must be satisfied.

$$G_1 = \frac{1}{2Z_0} \tag{4.7}$$

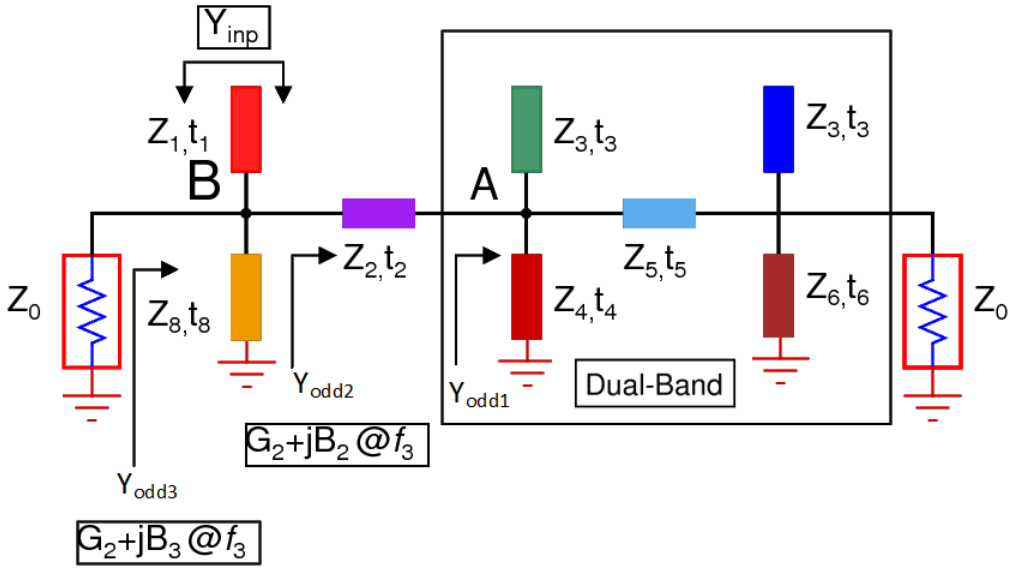

Fig 4.2. The odd mode equivalent of the proposed balun

The solution of (4.7) leads to the expression shown in (4.8) for the characteristic admittance Y_5 i.e. inverse of characteristic impedance Z_5. Here, the characteristic impedances Z_3 and Z_6 are considered as free variables. This helps in getting the realizable value of characteristic impedance Z_5. The other unknown i.e. characteristic impedance Z_4 can be calculated as elaborated in subsection 4.3.2 i.e. the even-mode analysis. Now, using these values of Z_4 and Z_5, the input impedance Y_{odd1} is calculated at the third arbitrary frequency, let say f_3 ($u = f_3/f_1$), in the form of (4.9). The same can also be evaluated using a simulation tool.

$$Y_5 = \frac{[-2Y_3 \tan^2 t + 2Y_6] \pm \sqrt{[-2Y_3 \tan^2 t + 2Y_6]^2 - 4[1+2\tan^2 t][2Y_3 Y_6 \tan^2 t - Y_3^2 \tan^4 t - Y_6^2 - Y_0^2 \tan^2 t]}}{2[1+2\tan^2 t]} \quad (4.8)$$

$$Y_{odd1}@f_3 = G_{num} + j\, B_{num} \quad (4.9)$$

To make the design work at f_3, a transmission line with characteristic impedance Z_2 and electrical length t_2 is added in the odd-mode equivalent of the dual-band balun. Now the real part of the input admittance Y_{odd2} needs to remain equal to the source admittance at f_3. Following equations govern the described procedure.

$$Z_2 = Z_0 \quad (4.10)$$

$$Y_{odd2}@f_3 = G_2 + j\, B_2 \quad (4.11)$$

where,

$$G_2 = \frac{[Y_2 G_1][Y_2 - B_1 \tan ut_2] + [Y_2 G_1 \tan ut_2][B_1 + Y_2 \tan ut_2]}{[Y_2 - B_1 \tan ut_2]^2 + G_1^2 \tan^2 ut_2} \quad (4.12)$$

$$B_2 = \frac{[Y_2][Y_2 - B_1 \tan ut_2][B_1 + Y_2 \tan ut_2] - [Y_2 G_1^2 \tan ut_2]}{[Y_2 - B_1 \tan ut_2]^2 + G_1^2 \tan^2 ut_2} \quad (4.13)$$

And again, $$G_2 = \frac{1}{2Z_0} \quad (4.14)$$

The expression (4.12) and (4.14) will provide the electrical length t_2 of the transmission line. Further, a combination of two stubs is added in the design at *node B* (as shown in Fig. 4.2) to offer infinite impedance at the same point for the signals at f_1 and f_2. The same can be described from (4.15).

$$Y_{inp} = \frac{Y_8}{j \tan t_8} - \frac{Y_1 \tan t_1}{j} = 0 \quad (4.15)$$

The effective admittance looking towards point *B* is now Y_{odd3} at f_3 which will reflect the changes only in imaginary part of Y_{odd3} as expressed as (4.16).

$$Y_{odd3}@f_3 = G_2 + j\,B_3 \tag{4.16}$$

And the imaginary part must be negligible to match the input admittance with the source admittance Y_0. Hence,

$$B_3@f_3 = B_2 + Y_1 \tan ut_1 - Y_8 \cot ut_8 = 0 \tag{4.17}$$

Now using (4.13), (4.15) and (4.17), the impedance of the stubs can be calculated for any specific electrical length.

4.3.2 Even Mode Analysis:

As mentioned earlier, the even-mode analysis is required for the determination of Z_4. The input admittance of dual band section i.e. Y_{even}, as shown in Fig. 4.3, can be written as

$$Y_{even} = jY_3 \tan t + jY_4 \tan t + \frac{\frac{1}{Y_3Y_5Y_6} + j\frac{1}{Y_0}\tan t\left[\frac{1}{Y_3}+\frac{1}{Y_5}+\frac{1}{Y_6}\right]}{\frac{1}{Y_3Y_5Y_6} - \frac{1}{Y_5}\tan t\left[\frac{\tan t}{Y_0Y_6}+\frac{\tan t}{Y_0Y_3}-j\frac{1}{Y_3Y_6}\right]} \tag{4.18}$$

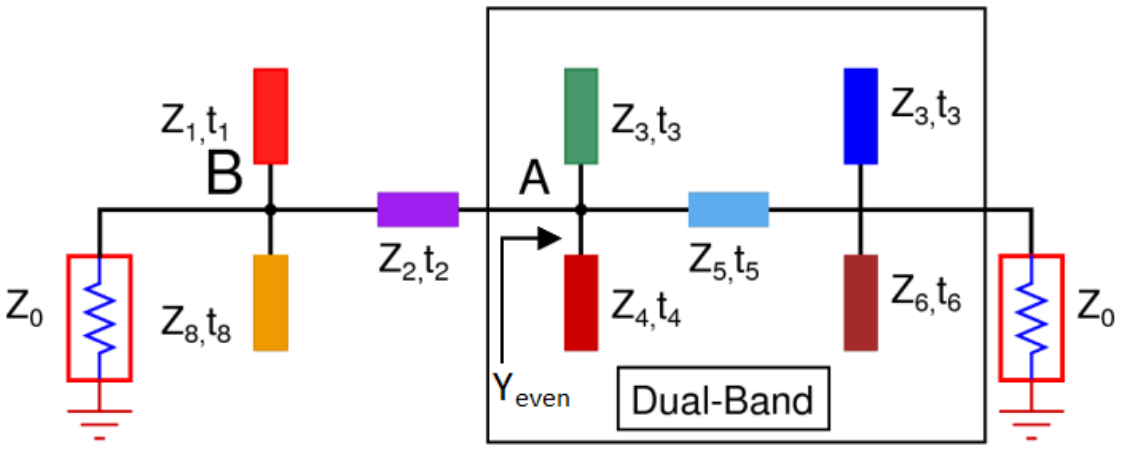

Fig 4.3. The even mode equivalent of the proposed balun

Referring (4.3), the real and imaginary part of (4.18) must be zero. Y_{even} can be expressed as (4.19) in terms of real and imaginary parts where imaginary part is

expressed as in (4.20) and equating this to zero will result in the unknown characteristic impedance Z_4.

$$Y_{even} = G_{even} + j\, B_{even} \tag{4.19}$$

$$B_{even} = Y_3 \tan t + Y_4 \tan t + \frac{\frac{1}{Y_0}\tan t\left[\frac{1}{Y_3}+\frac{1}{Y_5}+\frac{1}{Y_6}\right]\left[\frac{1}{Y_0Y_3Y_6}-\frac{\tan^2 t}{Y_0Y_5Y_6}-\frac{\tan^2 t}{Y_0Y_3Y_5}\right]-\frac{\tan t}{Y_3^2Y_5^2Y_6^2}}{\frac{1}{Y_0^2}\left[\frac{1}{Y_3Y_6}-\frac{\tan^2 t}{Y_5Y_6}-\frac{\tan^2 t}{Y_3Y_5}\right]^2+\frac{\tan^2 t}{Y_3^2Y_5^2Y_6^2}} \tag{4.20}$$

$$B_{even} = 0 \tag{4.21}$$

4.4 The Design Procedure and the Design Example:

The design procedure can be written in easy steps as:

- Measure the electrical length of the transmission lines with an electrical length t_3, t_4, t_5, and t_6 from (4.1) as per the desired frequency ratio for dual band operation.
- The characteristic impedance Z_5 can be computed as $Z_5 = 1/Y_5$. Y_5 can easily be found from (4.8). Use values of Z_3 and Z_6 as free variable here.
- Use (4.21) to find the value of Z_4. This completes the design for dual-band balun section.
- The electrical length of the transmission line having a characteristic impedance Z_5 can be calculated from (4.12) and (4.14) together. The characteristic impedance will be equal to the source impedance.
- Finally, the electrical length of remaining two stubs (with characteristic impedance Z_1 and Z_8) must be chosen to keep the null at node B at dual-bands. This can be computed from (4.1) and the characteristic impedances can be computed from (4.13), (4.15) and (4.17). This will provide a complete architecture for tri-band balun.

Now, a prototype is designed based on this elaborated design procedure. All the port impedances i.e. Z_0 are considered same and are 50Ω. A length of t_i = 60° is computed for i = 3, 4, 5, 6 and n = 1 for the dual band operation. The characteristic impedance Z_5 = 74.074Ω and Z_4 = 34.50Ω are calculated from (4.8) and (4.21) using Z_3 =

60Ω and Z_6 = 50Ω as free variables. Keeping Z_2 = 50Ω as explained in section 4.3, t_2 = 13.63° using (4.12) and (4.14). Afterwards, Z_1 and Z_8, keeping electrical length same, i.e. $t_1 = t_8$ = 60°, the impedances Z_1 = 57.8Ω and Z_8 = 19.27Ω are computed using (4.13), (4.15) and (4.17).

For the sake of realization of the proposed approach at different frequency ratios, characteristic impedances (in Ω) and electrical lengths (in °) of each transmission line is computed at 1.2/1.8/2.2 GHz and shown in Table 4.1.

TABLE 4.1 CALCULATED PARAMETERS OF ANOTHER EXAMPLE

$f_1 = 1.2\ GHz, f_2 = 1.8\ GHz, and\ f_3 = 2.2\ GHz$							
$\boldsymbol{Z_1}$	90.05	$\boldsymbol{Z_3}$	62.6	$\boldsymbol{Z_5}$	46.0	$\boldsymbol{Z_8}$	83.9
$\boldsymbol{t_1}$	72	$\boldsymbol{t_3}$	72	$\boldsymbol{t_5}$	72	$\boldsymbol{t_8}$	72
$\boldsymbol{Z_2}$	50	$\boldsymbol{Z_4}$	33.9	$\boldsymbol{Z_6}$	72.9		
$\boldsymbol{t_2}$	131.9	$\boldsymbol{t_4}$	72	$\boldsymbol{t_6}$	72		

4.5 Simulation and Measurement Results:

Based on the design procedure the tri-band balun is designed and optimized in a simulation environment and the results are well matched with the expected performance at 1.0/2.0/2.5 GHz. Momentum simulator in the microwave mode of Keysight ADS is done and the simulation results for S-parameters are shown in Fig. 4.4 and for phase difference between output ports is shown in Fig. 4.6.

The designed tri-band balun is then implemented on Rogers 5880 substrate with the substrate thickness of the board being 1.575mm, ε_r = 2.2 and tanδ = 0.0009. The board is laminated with copper cladding of 35 μm on both sides. The measurement results have been superposed in Figs. 4.5 and 4.6 and are also listed in Table 4.2. The measured results clearly indicates good matching and insertion loss along with the phase deviation within ±5° at the design frequencies. A slight shift in the frequencies can

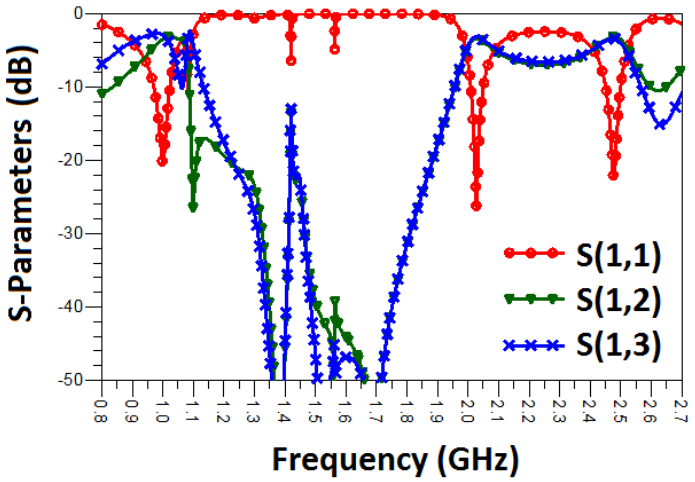

Fig. 4.4. S-Parameter EM Simulation Results

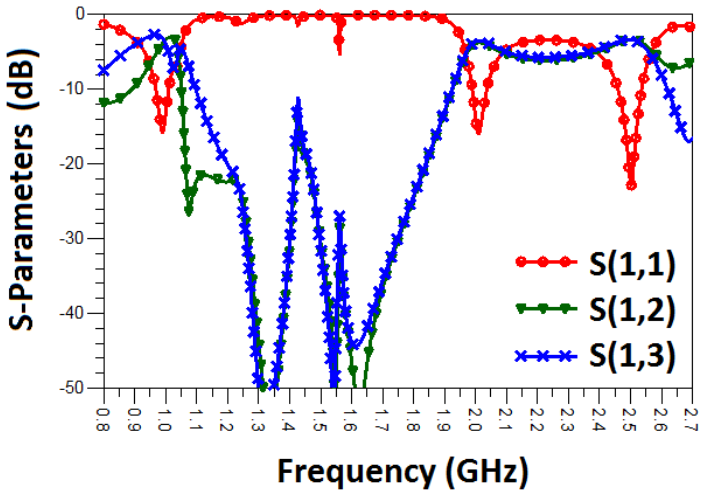

Fig. 4.5. S-Parameter Measurement Results

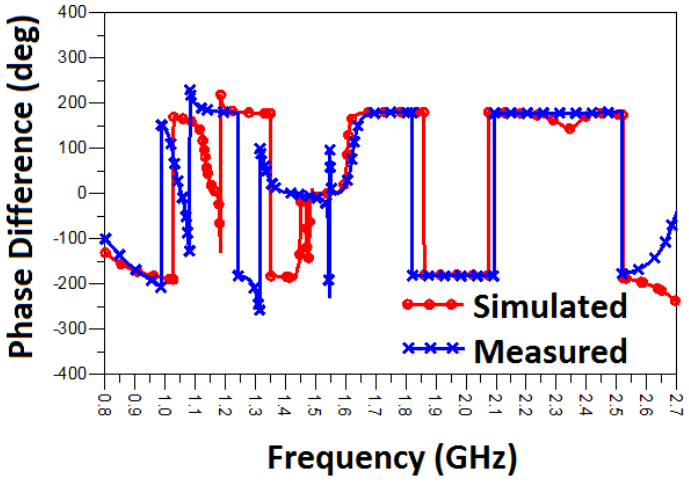

Fig. 4.6. Phase difference between port 2 and port 3

be observed in the figure and that is due to the in-house fabrication. Table 4.3 presents a comparison with the state-of-the-art dual- and tri-band baluns. It is evident that the tri-band design proposed in this chapter achieves significantly improved performance over the existing tri-band balun. It also exhibits comparable performance to the existing dual-band baluns. It can thus be concluded that the proposed design strategy substantially advances the state-of-the-art in the multi-band balun. The fabricated device is shown in Fig. 4.7.

TABLE 4.2 MEASUREMENT RESULTS OF THE PROTOTYPE

Frequency (GHz)	S_{11} (dB)	S_{21} (dB)	S_{31} (dB)	Phase Difference (°)
$f_1 = 0.99$	-15.7	-3.3	-3.1	-184.2
$f_2 = 2.00$	-16.0	-3.7	-3.4	-180.1
$f_3 = 2.50$	-22.8	-3.3	-3.3	-175.2

TABLE 4.3 COMPARISION WITH THE STATE-OF-THE-ART TECHNIQUES

Ref	Max Freq Shift	S_{11} (dB) Max	S_{21} (dB) Min	S_{31} (dB) Min	Max Phase Deviation
[15]	~500 MHz	-13.24	-6.55	-6.54	<5°
[14]	~170 MHz	-16.0	-3.7	-3.7	<1°
[24]	~120 MHz	-12.5	-6	-6	<10°
[This Work]	~10 MHz	-15.2	-3.7	-3.4	<5°

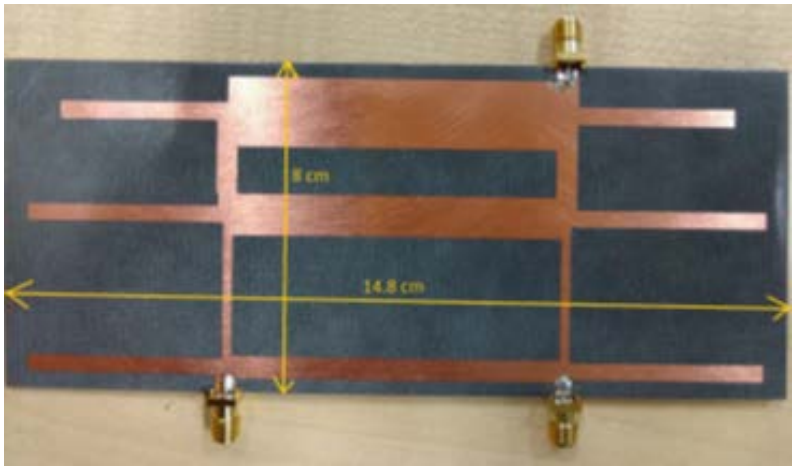

Fig. 4.7. The fabricated Prototype

4.6 Conclusion:

A new structure for a tri-band balun is proposed and the concept is validated with the prototype working at 1/2/2.5 GHz. A systematic design procedure with closed form expressions has been developed that has the ability to provide easy design and development at arbitrarily chosen frequencies. The free design variables provide the design an added degree of freedom. It has been demonstrated that the achieved results are substantially improved when compared with the existing tri-band balun design [24].

CONCLUSION

The motivation behind designing the baluns is its increasing demand in today's RF/Microwave, TV receivers, and modern era telecommunication networks. These devices are extensively required for impedance matching, DC isolation, and matching the single ended port with differential ended ports. It is well known that the flux coupled type baluns are good for the isolation, but transmission line type baluns are used only for a higher range of frequencies and wideband operations. Flux coupled transformers are commonly used for IF applications while transmission line transformers are used for RF and Local Oscillator applications. The requirement is henceforth, a device which can serve the purpose at multiple frequencies due to multi band communication networks.

In this thesis, three architectures have been proposed to provide a wideband balun, to improve the isolation, and provide a tri-band balun working at three arbitrary frequencies to cater the need of modern era communication network. The design analysis is provided in detail, with closed form equations to calculate all the required parameters of the proposed architecture. The availability and conditions of the free variables are discussed in the analysis as well. A prototype for a wideband balun working at 2 GHz, a wideband balun with isolation at its output ports at 1.8 GHz, and a tri-band balun working at 1/2/2.5 GHz are fabricated. The results of these prototypes are compared with the simulation results and are represented in the respective chapters. All the EM simulation results matched very well with the measurement results of the prototype.

BIBLIOGRAPHY

[1] P. Kim, G. Chaudhary, and Y. jeong, “Analysis and design of a branch-line balun with high-isolation wideband characteristic,” *Wiley Microw. Opt. Technol. Lett.*, vol. 57, no. 5, pp. 1098–2760, May 2015.

[2] J. Shao, R. Zhou, C. Chen, X.-H. Wang, H. Kim, and H. Zhang, "Design of a wideband balun using parallel strips," *IEEE Microw. Wireless Compon. Lett*., vol.23, no.3, pp.125-127, Mar. 2013.

[3] Y. Zhichao, L. Shanshan, B. Feng, Z. Mingmin, Z. Peng, and W. Wenfeng, "A novel wideband balun with a CPW power divider," *IEEE Asia Pacific Intern. Symp. On Electromag. Compat.*, Shenzhen, pp.652-655, 2016.

[4] W. Feng, and W. Che, "Wideband balun bandpass filter based on a differential circuit," *IEEE MTT-S International Micro. Symp. Digest*, Montreal, QC, pp.1-3, 2012.

[5] W. M. Fathelbab and M. B. Steer, “New classes of miniaturized planar Marchand baluns,” *IEEE Trans. Microw. Theory Tech*., vol. 53, no. 4, pp. 1211–1220, Apr. 2005.

[6] I. Piekarz, J. Sorocki, S. Gruszczynski, and K. Wincza, “Input match and output balance improvement of Marchand balun with connecting line,” *IEEE Microw. Wireless Compon. Lett*., vol. 24, no. 10, pp. 683–685, Oct. 2014.

[7] K. S. Ang, and I. D. Robertson, ”Analysis and design of impedance transforming planar Marchand baluns,” *IEEE Trans. on Microw. Theory and Tech.*, vol. 49, no. 2, pp. 402-406, Feb. 2001.

[8] K. S. Ang, Y. C. Leong, and C. H. Lee, ”Analysis and design of miniaturized lumped-distributed impedance-transforming baluns,” *IEEE Trans. on Microw. Theory and Tech*., vol. 51, no. 3, pp. 1009-1017, Mar. 2003.

[9] H.-R. Ahn and T. Itoh, “New isolation circuits of compact impedance transforming 3-dB baluns for theoretically perfect isolation and matching,” *IEEE Trans. Microw. Theory Tech*., vol. 58, no. 12, pp. 3892–3902, Dec. 2010.

[10] H. Ahn and T. Itoh, ”Isolation circuit of impedance-transforming 3-dB compact baluns for near perfect output matching and isolation,” *IEEE MTT-S International Microw. Symp. Digest*, Anaheim, CA, May 2010.

[11] M. Zhou, J. Shao, B. Arigong, H. Ren, J. Ding, and H. Zhang, “Design of microwave baluns with flexible structures,” *IEEE Microw. Wireless Compon. Lett*., vol. 24, no. 10, pp. 695–697, Oct. 2014.

[12] H. Zhang, Y. Peng, and H.Xin, “A tapped stepped-impedance balun with dual-band operations,” *IEEE Antennas Wireless Propag. Lett.*, vol.7, pp. 119–122, May 2008.

[13] A. L. Shen, M. Zhou, B. Arigong, J. Shao, H. Ren, J. Ding, R. Zhou, and H. Zhang, “Dual-band baluns with flexible frequency ratios,” *IET Electronic Lett.*, vol. 50, no. 17, pp. 1213–1214, Aug. 2014.

[14] A. L. Shen, M. Zhou, B. Arigong, J. Shao, H. Ren, J. Ding, R. Zhou and H. Zhang, ”Dual-band balun with flexible frequency ratios,” *Electronic Lett.*, vol. 50, no. 17, pp. 1213-1214, Aug. 2014.

[15] H. Zhang and H. Xin, ”Dual-band branch-line balun for millimeter-wave applications,” *IEEE MTT-S International Microw. Symp. Digest*, Boston, MA, pp. 717-720, June 2009.

[16] L. K. Yeung, and K. L. Wu, ”A dual-band coupled line balun filter,” *IEEE Trans. on Microw. Theory and Tech.*, vol. 55, no. 11, pp. 2406-2411, Nov. 2007.

[17] X. Gao, L. K. Yeung, and K. L. Wu, ”A dual-band balun using coupled stepped-impedance coupled line resonators,” *IEEE International Conf. on Microw. and Millimeter Wave Tech.*, Nanjing, pp. 39-42, 2008.

[18] X. Gao, L. K. Yeung, and K. L. Wu, ”A dual-band balun using partially coupled stepped-impedance coupled line resonators,” *IEEE Trans. on Microw. Theory and Tech.*, Vol 56, no 6, pp. 1455-1460, June 2008.

[19] Y. Wu, L. Yao, W. Zhang, W. Wang, and Y. Liu, ”A planar dual-band coupled line balun with impedance transformation and high isolation,” *IEEE Access*, vol 4, pp. 9689-9701, 2016.

[20] W. Zhang, Y. Wu, W. Wang, and X. Shen, ”Planar compact dual-band coupled line balun with high isolation,” *IEEE China Comm*., vol 14, no 2, pp. 40-48, Feb. 2017.

[21] H. Zhang, Y. Peng, and H. Xin, ”Design of dual-band balun with tapped stubs,” *IEEE Radio and Wireless Symp.*, Orlando, pp. 859-862, 2008.

[22] H. Zhang, J. Shao, S. Tan, and K. J. Chen, ”Design of dual-band coupled line balun,” *IEEE International Workshop on Antenna Technology*, Hong Kong, pp. 332-335, 2011.

[23] H. Zhang, and H. Xin, ”Dual-band balun with fully matched performance,” *IEEE Asia Pacific Microw. Conf.*, Macau, pp. 1-4, 2008.

[24] C. Y. Liou, and S. G. Mao, ”Triple-band marchand balun filter using coupled-line admittance inverter technique,” *IEEE Trans. on Microw. Theory and Tech.*, vol. 61, no. 11, pp. 3846-3852, 2013.

[25] M. A. Maktoomi, R. Gupta, M. H. Maktoomi, M. S. Hashmi and F. M. Ghannouchi, ”A generalized multi-frequency impedance matching technique,” *IEEE 16th Mediterranean Microw. Conf.*, Abu Dhabi, UAE, pp. 1-4, Nov. 2016.

[26] M. A. Maktoomi, M. Akbarpour, M. S. Hashmi, and F. M. Ghannouchi, ”A theorem for multi-frequency DC-feed network design,” *I EEE Microw. Wireless Compon. Lett*., vol. 26, no. 9, pp. 648-650, Sept. 2016.

[27] Y. Wu, L. Yao, W. Zhang, W. Wang and Y. Liu, "A Planar Dual-Band Coupled-Line Balun With Impedance Transformation and High Isolation," *IEEE Access*, vol. 4, pp. 9689-9701, 2016.